TITLE

Novel Orbits of Mercury, Venus and Mars Enabled using Low-Thrust Propulsion

AUTHOR NAMES AND AFFILIATIONS

Pamela Anderson
Advanced Space Concepts Laboratory, Department of Mechanical and Aerospace Engineering
University of Strathclyde
Level 4 Lord Hope Building
141 St James Road
Glasgow, United Kingdom
G4 0LT
pamela.c.anderson@strath.ac.uk
Phone: +44(0)141 444 8294
(Corresponding author)

Malcolm Macdonald
Advanced Space Concepts Laboratory, Department of Mechanical and Aerospace Engineering
University of Strathclyde
Level 4 Lord Hope Building
141 St James Road
Glasgow, United Kingdom
G4 0LT
malcolm.macdonald.102@strath.ac.uk
Phone: +44(0)141 548 2042

Chen-wan Yen
Mission Design and Navigation, Jet Propulsion Laboratory California Institute of Technology
4800 Oak Grove Drive
Pasadena, California, US
91109
chen-wan.l.yen@jpl.nasa.gov
Phone: +1 626 354 4899

AUTHOR BIOGRAPHIES

Pamela Anderson received a B.Eng (Hons) degree in Aero-Mechanical Engineering from the University of Strathclyde in 2009. Before joining the Advanced Space Concepts Laboratory at the University of Strathclyde in October 2009, where her research interests include mission analysis and design and Earth Observation. She also spent three months working within the Mission Design and Navigation Section at the Jet Propulsion Laboratory / California Institute of Technology as part of her PhD in 2012.

Malcolm Macdonald obtained a B.Eng in aeronautical engineering from the University of Glasgow in 2000. He then studied for his PhD at the University of Glasgow from 2000 – 2002, prior to gaining a research assistant post until December 2004. From 2005 – 2008 he worked at SciSys UK Ltd. on a range of European Space Agency missions throughout the project life cycle, progressing to become a senior member of technical staff leading a team working across non-linear dynamic systems and control, modelling and simulation and advanced mission and concept studies. He joined the Advanced Space Concepts Laboratory at the University of Strathclyde in 2008, where his research interests cover astrodynamics, mission analysis and design, spacecraft systems, including solar sailing and nano-spacecraft, and unmanned autonomous systems.

Dr. Chen-wan Yen is a graduate of MIT in nuclear physics. Since she joined JPL in 1973 she specialized in trajectory optimizations and designed many missions entailing complex gravity assists, electric propulsion or solar sail. She is the originator of the trajectory for Magellan, Cassini, Stardust and the upcoming Messenger missions.

ABSTRACT

Exploration of the inner planets of the Solar System is vital to significantly enhance the understanding of the formulation of the Earth and other planets. This paper therefore considers the development of novel orbits of Mars, Mercury and Venus to enhance the opportunities for remote sensing of these planets. Continuous acceleration is used to extend the critical inclination of highly elliptical orbits at each planet and are shown to require modest thrust magnitudes. This paper also presents the extension of existing sun-synchronous orbits around Mars. However, unlike Earth and Mars, natural sun-synchronous orbits do not exist at Mercury or Venus. This research therefore also uses continuous acceleration to enable circular and elliptical sun-synchronous orbits, by ensuring the orbit's nodal precession rate matches the planets mean orbital rate around the Sun, such that the lighting along the ground-track remains approximately constant over the mission duration. This property is useful both in terms of spacecraft design, due to the constant thermal conditions, and for comparison of images. Considerably high thrust levels are however required to enable these orbits, which are prohibitively high for orbits with inclinations around *90 degrees.* These orbits therefore require some development in electric propulsion systems before becoming feasible.

Keywords: Low-thrust propulsion, sun-synchronous orbits, critical inclination, Mars, Mercury, Venus

MANUSCRIPT

1. Introduction

Planetary observation is vital to gain an insight into the history of the Solar System and in turn the formulation of Earth, and can be used to determine whether extra-terrestrial habitable environments exist in the Solar System.

The Martian environment is of particular interest with recent missions including Mars Odyssey [1], Mars Express [2], Mars Reconnaissance Orbiter (MRO) [3], and the Mars Science Laboratory (MSL) [1]. Such missions have allowed a comprehensive view of Mars to be obtained through data of the Martian surface geology, mineral composition, subsurface structure, radiation environment and weather. However, additional significance has recently been placed on exploration of Mars with the reformulation of the Mars Exploration Program [4]. This program aims to assess both near-term mission concepts and longer-term foundations of program level architectures for future robotic exploration. As a result missions must be developed which are responsive to the scientific goals of both the National Research Council Planetary Decadal Survey [5] and the ESA Aurora Program [2].

Similarly, the NASA Vision and Voyages Decadal Survey for 2013 – 2022 has identified three themes for the future development of planetary science, within which the importance of investigating the evolution of the inner planets and their atmospheres is highlighted [5]. The importance of examining the chemistry, climates and geology of the inner planets is also outlined to lead to a better understanding of climate change on Earth [5]. The importance of further exploration of Mercury and Venus is therefore clear.

This paper develops novel orbits of Mars, Mercury and Venus to enable new and unique investigations and allow enhanced investigation into the surface, subsurface and atmospheres of these bodies.

Natural orbits typically used for remote sensing applications at Earth also exist at Mars. For example, sun-synchronous orbits, which have in the past been employed by spacecraft such as Mars Odyssey [1], MRO [6], and Mars Global Surveyor [7] and Molniya-like orbits with fixed values of the critical inclination [8], which can also offer benefits for remote sensing of Mars by allowing the spacecraft to spend a large amount of time over a region of interest as a result of apoareion dwell.

Similar to Mars, orbits inclined at the critical inclination also exist at Mercury and Venus, however the reciprocal of flattening of these planets is so low that natural perturbations are insufficient to generate sun-synchronous orbits. Investigation has therefore previously been conducted into the use of a solar sail to deliver a sun-synchronous orbit around Mercury [9].

This paper extends methods previously introduced by the authors for the extension of Earth orbits [10, 11] to; extend existing highly-elliptical orbits at Mars, Mercury and Venus; extend sun-synchronous orbits around Mars; and enable sun-synchronous orbits at Mercury and Venus where they are otherwise not possible, as such significantly enhancing the opportunities for remote sensing of these bodies.

---

[1] http://www.nasa.gov/mission_pages/msl/index.html Accessed 14 March 2013

[2] http://www.esa.int/Our_Activities/Human_Spaceflight/Exploration/Aurora_s_roadmap_to_Mars Accessed 14 March 2013

2. Mars

The work presented herein extends these natural orbits using continuous low-thrust propulsion to create a new set of Martian orbits for improved remote sensing, while maintaining the zero change in argument of periapsis condition essential to Molniya-like orbits. This is achieved firstly by developing a general perturbations solution, which is validated using a special perturbations solution.

These solutions can also be extended by the addition of a further element of continuous low-thrust directed out of the orbit plane to ensure that the rate of change of ascending node of the orbit matches the mean rotation of the Sun, and achieve sun-synchronous orbits with fixed critical inclinations and thus no rotation of the apsidal line. The development of such novel orbits therefore creates additional observation opportunities of the surface and atmosphere of Mars, allowing more accurate observations for possible future human exploration. One such example would be to enable a sun-synchronous HEO inclined at *90 degrees* to allow improved studies of the Martian Polar Regions.

Furthermore, these new orbits may be of use for communication relay for human missions or Unmanned Aerial Vehicles (UAVs) or detailed mapping of the Martian surface. The transition from single spacecraft exploration of Mars to fleet of vehicles both around Mars and on the Martian surface further highlights possible benefits of these novel orbits.

The importance of analyzing atmospheric and meteorological phenomena at Mars has also seen recent research into the development of multi-sun-synchronous orbits of Mars, which allow cycles of observation of the same area under illumination conditions which repeat after a periodicity multiple of the repetition of observation [12, 13].

2.1 Spacecraft Motion about an Oblate Body

At Earth the most dominant perturbation is the oblateness term, J_2, with a value of $1.082627x10^{-3}$. The harmonic coefficients J_3 and J_4 are around three orders of magnitude smaller than the J_2 term, with $J_3 = -2.53266x10^{-6}$, and $J_4 = -1.61962x10^{-6}$, and thus have a negligible effect on the determination of the critical inclination. At Mars, the J_2 perturbation is also dominant, with a value of $1.95545x10^{-3}$. However, zonal harmonics through to J_5 are only around two orders of magnitude lower than the J_2 perturbation, with values of $J_3 = 3.14498x10^{-5}$, $J_4 = -1.53774x10^{-5}$, and $J_5 = 9.0793x10^{-6}$, and so will have an impact on the determination of the critical inclination at Mars. As a result higher order terms must be taken into consideration in this instance.

Considering the gravitational potential of a body [14]

$$U(r,\beta,\lambda) = \frac{\mu}{r}\sum_{n=0}^{\infty}\sum_{m=0}^{\infty}\left(\frac{R_B}{r}\right)^n \left(C_{n,m}\cos(m\lambda) + S_{n,m}\sin(m\lambda)\right)P_{n,m}\sin\beta \qquad (1)$$

Where, U is the gravitational potential, r is the orbit radius, β is the declination of the spacecraft, λ is the geographical longitude, μ is the gravitational parameter of the body under consideration, R_B, is the radius of the body under consideration, Cn,m, and Sn,m are the harmonic coefficients of body potential, and Pn,m is the associated Legendre polynomials. For a body possessing axial symmetry the influence of periodic effects (tesseral and sectorial harmonics) can be neglected for most orbits. The gravitational potential may be written as

$$U(r,\beta)=\frac{\mu}{r}\left[1-\sum_{n=0}^{\infty}J_n\left(\frac{R_B}{r}\right)^n P_n\sin\beta\right] \tag{2}$$

Where, J_n, are the gravitational perturbations. Expanding Eq. (**2**), the gravitational potential becomes

$$\begin{aligned}U(r,\beta)=\frac{\mu}{r}[1&-J_2\frac{1}{2}\left(\frac{R_B}{r}\right)^2\left(3\sin^2(\beta)-1\right)\\&-J_3\frac{1}{2}\left(\frac{R_B}{r}\right)^3\left(5\sin^2(\beta)-3\right)\sin\beta\\&-J_4\frac{1}{8}\left(\frac{R_B}{r}\right)^4\left(3-30\sin^2(\beta)+35\sin^4(\beta)\right)\\&-J_5\frac{1}{8}\left(\frac{R_B}{r}\right)^4\left(63\sin^5(\beta)-70\sin^3(\beta)+15\sin(\beta)\right)\\&-....]\end{aligned} \tag{3}$$

Where

$$\sin(\beta)=\sin(i)\,\sin(u) \tag{4}$$

From Eq. (**4**), u is the argument of latitude defined as $(\theta+\omega)$. Including perturbations to the order of J_5 and using spherical triangle laws Eq. (**3**) becomes

$$\begin{aligned}U(r,\beta)=U_0+U_p=\frac{\mu}{r}&-J_2\frac{\mu R_B^{\,2}}{2r^3}\left(3\sin^2(i)\sin^2(\theta+\omega)-1\right)\\&-J_3\frac{\mu R_B^{\,3}}{2r^4}\left(5\sin^3(i)\sin^3(\theta+\omega)-3\sin(i)\sin(\theta+\omega)\right)\\&-J_4\frac{\mu R_B^{\,4}}{8r^5}\left(3-30\sin^2(i)\sin^2(\theta+\omega)+35\sin^4(i)\sin^4(\theta+\omega)\right)\\&-J_5\frac{\mu R_B^{\,5}}{8r^6}\left(63\sin^5(i)\sin^5(\theta+\omega)-70\sin^3(i)\sin^3(\theta+\omega)+15\sin(i)\sin(\theta+\omega)\right)\end{aligned} \tag{5}$$

Where, i is the orbit inclination, θ is the true anomaly, and ω is the argument of pericentre. The disturbing force components in the radial, transverse and normal directions are found by taking the partial derivatives of Eq. (5) with respect to r, u and i respectively as follows

$$R_{J_2}=\frac{\partial U_p}{\partial r} \tag{6}$$

$$T_{J_2}=\frac{\partial U_p}{r\partial u} \tag{7}$$

$$N_{J_2}=\frac{\partial U_p}{r\sin(u)\partial i} \tag{8}$$

This results in expressions for the perturbing accelerations in the radial, transverse and normal directions given in Eqs. (9) - (11) these expressions are extended further in Sections 2.2.1 and 2.3 to develop new highly elliptical and sun-synchronous orbits.

$$\begin{aligned}R_J=\frac{\mu R_B^2}{8r^7}&(-12J_2r^3+15J_4rR_B^2+\sin(i)\sin(\theta+\omega)(-48J_3r^2R_B+90J_5R_B^3+\sin(i)\sin(\theta+\omega)(6r(6J_2r^2-25J_4R_B^2)\\&+R_B\sin(i)\sin(\theta+\omega)(80J_3r^2-420J_5R_B^2+7R_B\sin(i)\sin(\theta+\omega)(25J_4r+54J_5R_B\sin(i)\sin(\theta+\omega))))))\end{aligned} \tag{9}$$

$$\begin{aligned}T_J=-\frac{R_B^2\mu\cos(\theta+\omega)\sin(i)}{8r^7}&(-12J_2r^2R_B+15J_5rR_B^3+\sin(i)\sin(\theta+\omega)(24J_2r^2-60J_4rR_B^2+5R_B\sin(i)\sin(\theta+\omega)\\&(6(2J_3r^2-7J_5R_B^2)+7R_B\sin(i)\sin(\theta+\omega)(4J_4r+9J_5R_B+7R_B\sin(i)\sin(\theta+\omega)))))\end{aligned} \tag{10}$$

$$N_J = -\frac{R_B^2 \mu \cos(i)}{8r^7}(-12J_3 r^2 R_B + 15J_5 R_B^3 + \sin(i)\sin(\theta+\omega)(24J_2 r^3 - 60J_4 r R_B^2 + 5R_B \sin(i)\sin(\theta+\omega) \\ (6(2J_3 r^2 - 7J_5 R_B^2) + 7R_B \sin(i)\sin(\theta+\omega)(4J_4 r + 9J_5 R_B \sin(i)\sin(\theta+\omega)))) \quad (11)$$

2.2 Elliptical Orbits

2.2.1 General Perturbations Solution

The equatorial bulge of Mars causes the argument of periapsis of the orbit to rotate; this effect is negated with orbits inclined at a critical inclination. The value of which is derived using the Gauss form of the Lagrange Planetary Equation for the rate of change of argument of periapsis [15].

$$\frac{d\omega}{d\theta} = \frac{r^2}{\mu e}\left[-R\cos(\theta) + T\left(1+\frac{r}{p}\right)\sin(\theta)\right] - \frac{r^3}{\mu p \tan(i)}\sin(\theta+\omega)N \quad (12)$$

Where, p is the semi-latus rectum, and e is the eccentricity of the orbit To obtain the value of the critical inclination Eqs. (**9**) - (**11**) are substituted into Eq. (**12**) and integrated analytically over one orbital revolution. Inserting orbital element values into the resulting formula, and setting this equal to zero, the resulting critical inclination is determined. For example, a 12-hr orbit with a pericentre altitude of *800 km* and apocentre altitude of *17,724 km* including perturbations to J_4 results in critical inclinations of *63.29 degrees* and *116.71 degrees*. Increasing the perturbations to include J_5 alters the critical inclination values to *63.24 degrees* and *116.76 degrees*, thus including the J_5 perturbation results in difference of less than *0.1%* from the J_4 results, and can therefore be neglected in order to significantly reduce the complexity of the solutions.

Equations (**9**) - (**11**) are simplified and low thrust terms added to allow the extension of the critical inclination. These low-thrust terms are added using the argument of periapsis control law [16] derived from the variational equation, given in Eq. (**12**), by consideration of the sine and cosine terms in this equation. Locally optimal control laws maximize the instantaneous rate of change of the argument of pericentre, and provide the thrust orientation in analytical form [16]. The locally optimal control law gives the distinct position of the orbit where the sign of the thrust is required to switch direction. The combined perturbations up to J_4 and low-thrust perturbations in each of the radial, transverse and out-of-plane directions are thus given by

$$R_{J+F_r} = \frac{\mu R_B^2}{8r^7}(-12J_2 r^3 + 15J_4 r R_B^2 + \sin(i)\sin(\theta+\omega)(-48J_3 r R_B + \sin(i)\sin(\theta+\omega)(6(6J_2 r^2 - 25J_4 R_B^2) \\ +5R_B \sin(i)\sin(\theta+\omega)(16J_3 r + 35J_4 R_B \sin(i)\sin(\theta+\omega))))) + F_r \operatorname{sgn}\left[\cos(\theta)\right] \quad (13)$$

$$T_{J+F_t} = \frac{R_B^2 \mu \cos(\theta+\omega)\sin(i)}{2r^6}(3J_3 r R_B - \sin(i)\sin(\theta+\omega) \\ (6J_2 r^2 - 15J_4 R_B^2 + 5R_B \sin(i)\sin(\theta+\omega)(3J_3 r + 7J_4 R_B \sin(i)\sin(\theta+\omega)))) + F_t \operatorname{sgn}\left[\sin\theta\right] \quad (14)$$

$$N_{J+F_n} = \frac{R_B^2 \mu \cos(i)}{2r^6}(3J_3 r R_B - \sin(i)\sin(\theta+\omega) \\ (6J_2 r^2 - 15J_4 R_B^2 + 5R_B \sin(i)\sin(\theta+\omega)(3J_4 r + 7J_4 R_B \sin(i)\sin(\theta+\omega)))) + F_n \operatorname{sgn}\left[\sin(\theta+\omega)\right] \quad (15)$$

Equations (**13**) - (**15**) are again substituted into Eq. (**12**) and integrated over one orbital revolution. The resulting equation for the change in argument of pericentre over the orbit is made up of an Earth gravity term to the order of J_4, a radial acceleration term and a transverse acceleration term, given by Eqs. (**16**) - (**19**).

$$\left(\Delta\omega\right)_0^{2\pi} = \left(\Delta\omega\right)_J + \left(\Delta\omega\right)_{F_r} + \left(\Delta\omega\right)_{F_t} \tag{16}$$

$$\begin{aligned}\left(\Delta\omega\right)_J = \frac{3\pi R_B^2}{512a^4 e\left(-1+e^2\right)^4}\big(&e(384a^2\left(-1+e^2\right)^2 J_2 - 135\left(4+5e^2\right)J_4 R_B^2 + 20(32a^2\left(-1+e^2\right)^2 J_2 \\ &-\left(52+63e^2\right)J_4 R_B^2)\cos\left(2i\right) - 35\left(28+27e^2\right)J_4 R_B^2\cos\left(4i\right)) \\ &+10eJ_4 R_B^2(-6+5e^2+4\left(-2+7e^2\right)\cos\left(2i\right)+7\left(2+9e^2\right)\cos\left(4i\right))\cos\left(2\omega\right) \\ &+16a\left(-1+e^2\right)J_3 R_B(-1-3e^2-4\cos\left(2i\right)+5\left(1+7e^2\right)\cos\left(4i\right))\csc\left(i\right)\sin\left(\omega\right)))\end{aligned} \tag{17}$$

$$\begin{aligned}\left(\Delta\omega\right)_{F_r} = \frac{1}{e\mu}2a^2 F_r(&-2+2e^2-4e\sqrt{-1+e^2}\,\mathrm{Arctanh}\left[\frac{-1+e}{\sqrt{-1+e^2}}\right] \\ &-e\sqrt{-1+e^2}\,\ln\left[\frac{1-e}{\sqrt{-1+e^2}}\right]+e\sqrt{-1+e^2}\,\ln\left[\frac{-1+e}{\sqrt{-1+e^2}}\right])\end{aligned} \tag{18}$$

$$\left(\Delta\omega\right)_{F_t} = -\frac{4a^2\left(-2+e^2\right)F_t}{e\mu} \tag{19}$$

Equation (**16**) is set equal to zero and solved for the acceleration required to achieve any value of critical inclination for any given orbit. In this case, the radial and transverse components of acceleration are not equal, and no out-of-plane element is included, as this does not always produce a reduction in the required acceleration magnitude over the individual accelerations and the addition of the normal acceleration adds significant complexity to the analytical expressions; this is explained in more detail in [10].

The resulting acceleration magnitudes are shown for a variety of orbit periods between 6 and 24 hours to achieve inclinations between *5* and *175 degrees* for a constant periapsis altitude of *800 km* to compensate for the drift in argument of pericentre caused by the perturbations to the order of J_4. The required acceleration to maintain the zero change in argument of perigee condition for a variety of orbit periods and inclinations are shown in Figure 1, and the corresponding Δv per orbit is shown in Figure 2, for an argument of pericentre value of *270 degrees*. It is noted that the acceleration magnitude is dependent on the value assigned to the argument of periapsis, however considering the results for an argument of pericentre of *0 degrees* shows a very small difference between the required acceleration from a value of *270 degrees*.

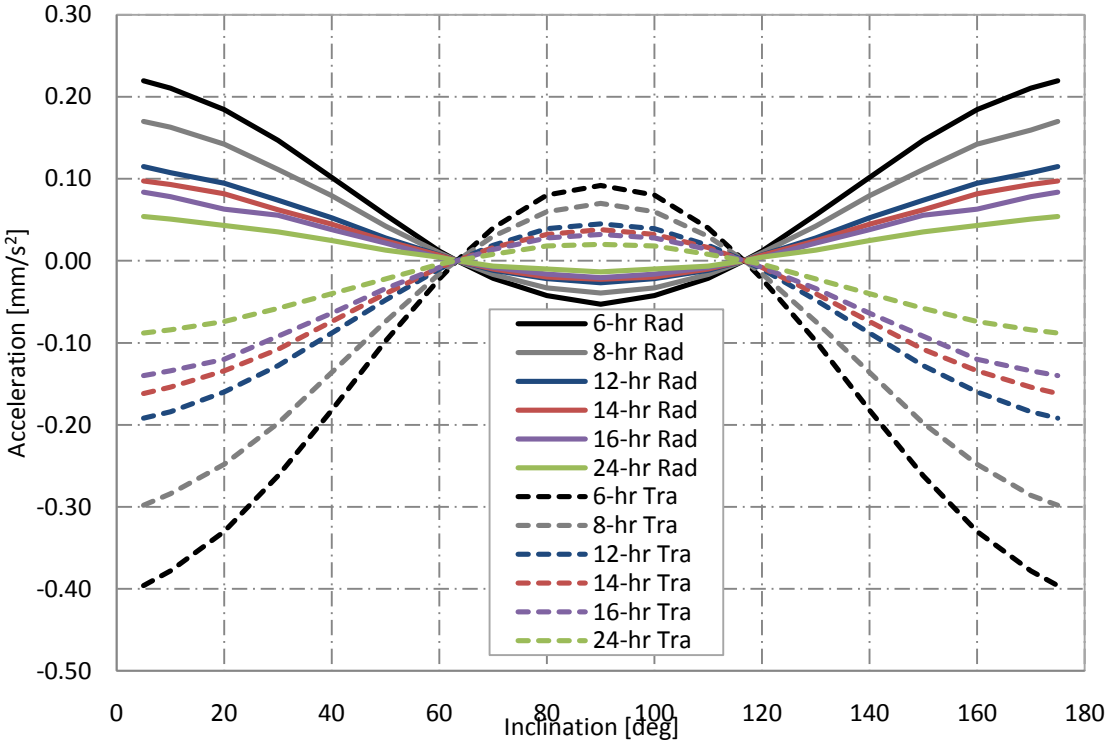

Figure 1 Required radial and transverse acceleration for the extension of the critical inclination at Mars

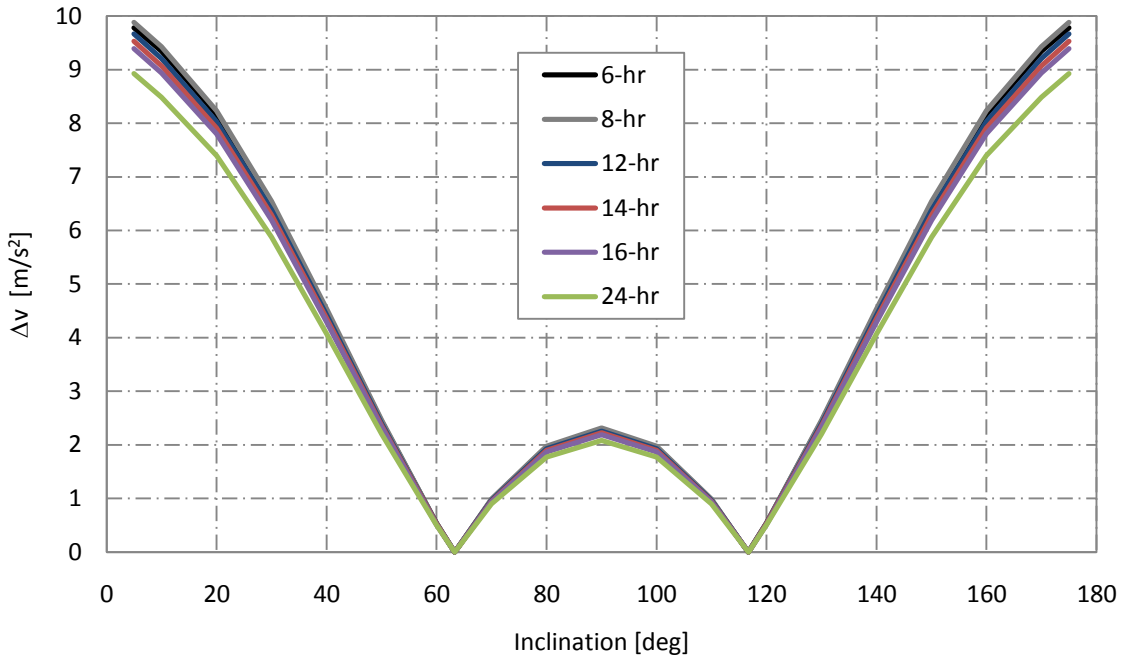

Figure 2 Required Δv per orbit for the extension of the critical inclination at Mars

Figure 1 shows the required acceleration in the radial and transverse directions to alter the critical inclination to a wide range of possible values for the given orbit. It is shown that as is to be expected, as the orbit period increases, the total acceleration magnitude decreases. Considering a 12 h orbit with an inclination of *90 degrees* requires a total acceleration of *0.05 mm/s*^{2}, consisting of *-0.027* and *0.045 mm/s*^{2} in the radial and transverse directions. Corresponding to *27* and *45 mN* of thrust respectively for a 1-ton spacecraft, which could be provided by NASA's Solar Electric Propulsion Application Readiness (NSTAR) thruster which is capable of providing between *20* and *94 mN* of thrust [17].

2.2.2 Special Perturbations Solution

Analytical solutions are verified using a special perturbations solution. This numerical model propagates the position of the spacecraft using a set of Modified Equinoctial Elements [18] using an explicit variable step size Runge-Kutta (4,5) formula, the Dormand-Prince pair [19]. Results are shown for the orbital elements for five revolutions of a 12 h orbit with *90 degree* inclination and *270 degree* argument of pericentre in Figure 3. These results show that although the semi-major axis, eccentricity and argument of pericentre oscillate over each orbital revolution, these elements return to the original value after each orbit. It is also shown that there are no changes experienced by inclination and ascending node angle.

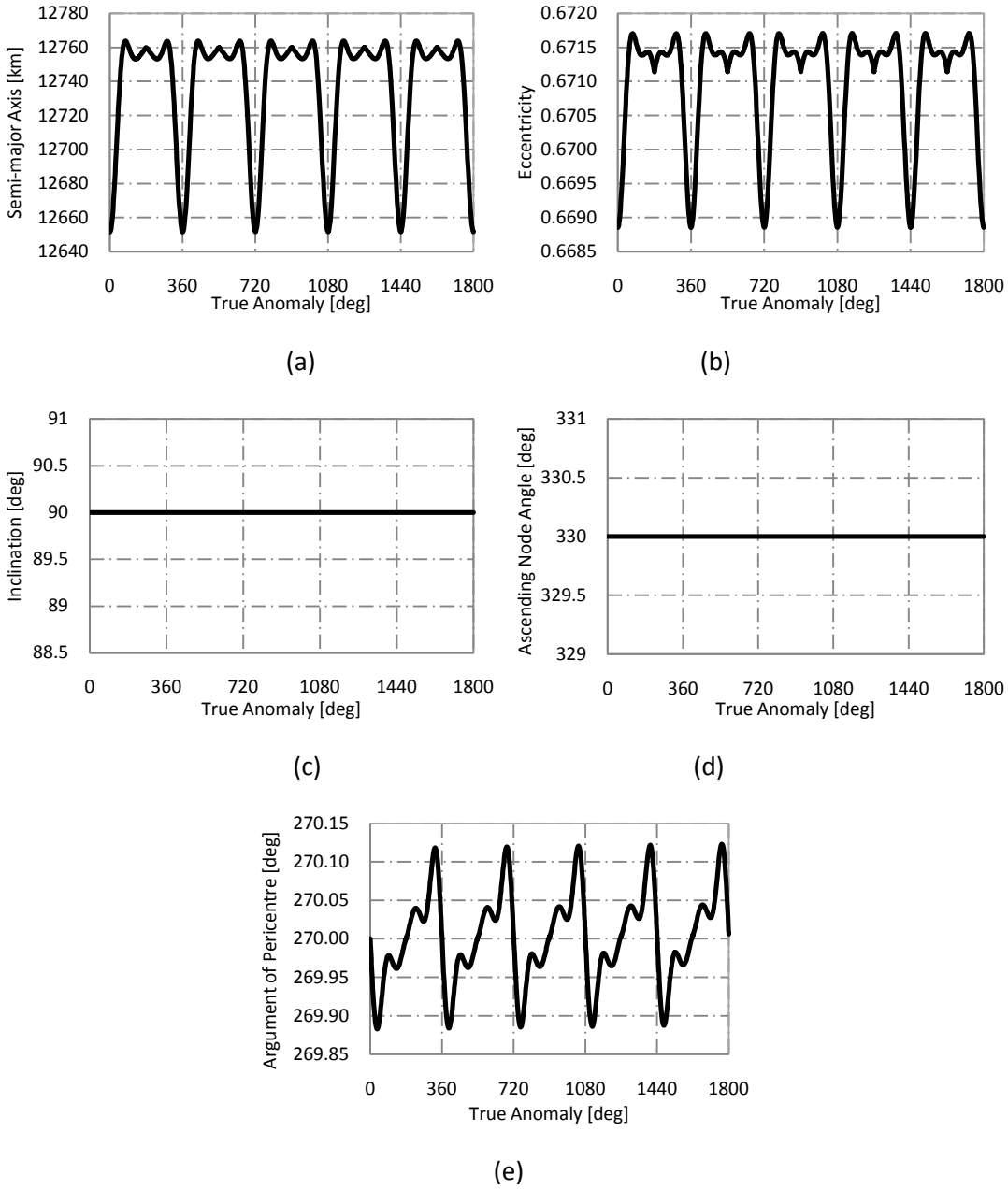

Figure 3 Oscillation of orbital elements over five orbital revolutions of a 12 h, *90 degree* inclination orbit at Mars (*270 degree* argument of periapsis) (a) Semi-major axis (b) Eccentricity (c) Inclination (d) Ascending node angle (e) Argument of pericentre

2.3 Sun-synchronous Orbits

In addition to the extension of the critical inclination, continuous low-thrust propulsion can also be used to extend existing sun-synchronous orbits to allow free selection of the orbit inclination and altitude. A sun-synchronous orbit requires the rate of change of the ascending node to match the motion of the mean Sun (*2π/686.429 rad/day*). The ascending node angle can also be described by the Gauss form of the variational equations using classical orbital elements [15].

$$\frac{d\Omega}{d\theta} = \frac{r^3}{\mu p \sin(i)} \sin(\theta + \omega) N \tag{20}$$

Eq. (**15**) is substituted into Eq. (**20**) and is again integrated over one revolution to give the change in ascending node over one orbit. In this case, as an out-of-plane acceleration is applied which is dependent on the argument of latitude, two solutions exist for an argument of pericentre equal to *0* and *270 degrees*, which give the maximum and minimum solutions. This is again explained in more detail in [10]. This change in ascending node over one orbit is given by Eq. (**21**).

$$(\Delta\Omega)_0^{2\pi} = (\Delta\Omega)_J + (\Delta\Omega)_{F_n} \tag{21}$$

Where,

$$(\Delta\Omega)_J = \frac{3\pi R_B^2}{32a^4\left(-1+e^2\right)^4}(\cos(i)(-32a^2\left(-1+e^2\right)^2 J_2 + 5\left(2+3e^2\right)J_4 R_B^2 + 35\left(2+3e^2\right)J_4 R_B^2 \cos(2i)) \tag{22}$$
$$-5e^2 J_4 R_B^2 (5\cos(i) + 7\cos(3i))\cos(2\omega) - 2ae\left(-1+e^2\right)J_3 R_B(\cos(i) + 15\cos(3i))\csc(i)\sin(\omega))$$

$$(\Delta\Omega)_{F_n,\omega=0} = -\frac{4a^2 F_n \cos(\omega)\cot(i)}{\mu} \tag{23}$$

$$(\Delta\Omega)_{F_n,\omega=270} = -\frac{a^2 F_n \csc(i)}{\sqrt{-1+e^2}\,\mu}(4\sqrt{-1+e^2} + 2e^2\sqrt{-1+e^2} \tag{24}$$
$$-12e\,\text{ArcTanh}\left[\frac{-1+e}{\sqrt{-1+e^2}}\right] - 3e\ln\left[\frac{1-e}{\sqrt{-1+e^2}}\right] + 3e\ln\left[\frac{-1+e}{\sqrt{-1+e^2}}\right]\sin(\omega))$$

Switching the rate of change of ascending node angle per rotation to per second and re-arranging, the two solutions for the change in ascending node per second for argument of periapsis equal to *0* and *270 degrees* respectively, are

$$(\Delta\Omega)_{\omega=0} = \frac{\sqrt{\mu}}{2\sqrt{a^3}\pi}(\frac{4a^2 F_n \cos(\omega)\csc(i)}{\mu} + \frac{1}{(32a^4\left(-1+e^2\right)^4)}3\pi R_B^2(\cos(i)(-32a^2\left(-1+e^2\right)^2 J_2 + 5\left(2+3e^2\right)J_4 R_B^2 \tag{25}$$
$$+35\left(2+3e^2\right)J_4 R_B^2\cos(2i)) - 5e^2 J_4 R_B^2(5\cos(i) + 7\cos(3i))\cos(2\omega)$$
$$-2ae\left(-1+e^2\right)J_3 R_B(\cos(i) + 15\cos(3i))\csc(i)\sin(\omega)))$$

$$(\Delta\Omega)_{\omega=270} = \frac{\sqrt{\mu}}{2\sqrt{a^3}\pi}(\frac{-1}{(\sqrt{-1+e^2}\,\mu)}a^2 F_n \csc(i)(4\sqrt{-1+e^2} + 2e^2\sqrt{-1+e^2} - 12e\,\text{ArcTanh}\left[\frac{-1+e}{\sqrt{-1+e^2}}\right]$$
$$-3e\ln\left[\frac{1-e}{\sqrt{-1+e^2}}\right] + 3e\ln\left[\frac{-1+e}{\sqrt{-1+e^2}}\right])\sin(\omega) + (\frac{1}{(32a^4\left(-1+e^2\right)^4)}) \tag{26}$$
$$3\pi R_B^2(\cos(i)(-32a^2\left(-1+e^2\right)^2 J_2 + 5\left(2+3e^2\right)^2 J_2 + 5\left(2+3e^2\right)J_4 R_B^2$$
$$+35\left(2+3e^2\right)J_4 R_B^2\cos(2i)) - 2ae\left(-1+e^2\right)J_3 R_B(\cos(i) + 15\cos(3i))\csc(i)\sin(\omega)))$$

2.3.1 Circular Sun-synchronous Orbits

Firstly, considering the extension of circular orbits, the acceleration magnitude directed out of the orbit plane to achieve free-selection of the inclination for a range of orbit altitudes is given in Figure 4, and the corresponding Δv per orbit is also shown in Figure 5.

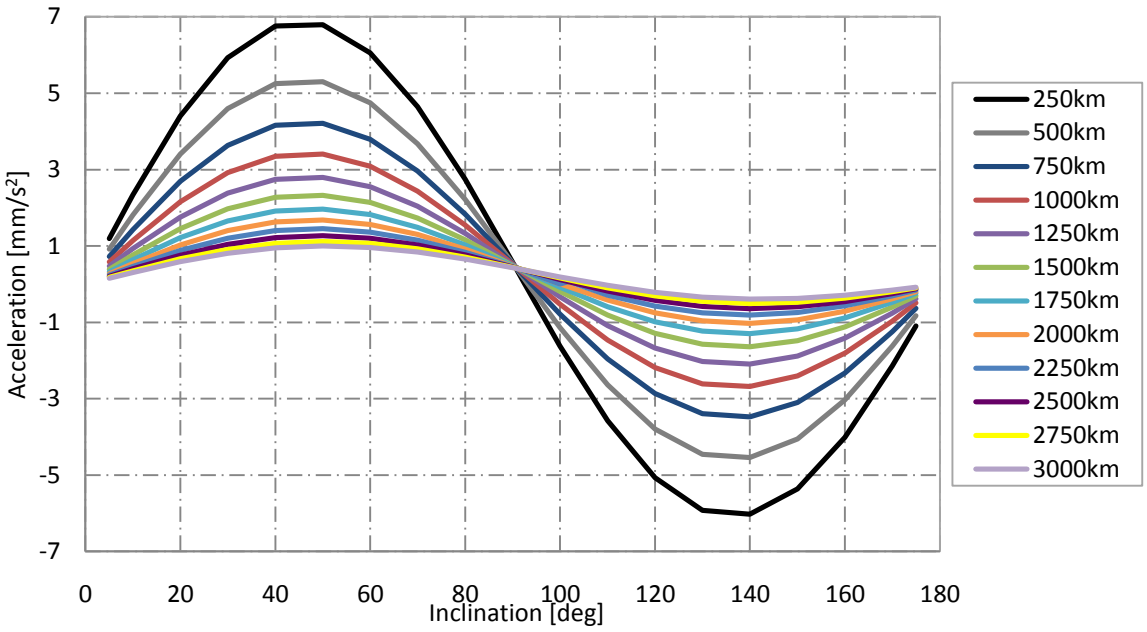

Figure 4 Required normal acceleration for the extension of circular sun-synchronous orbits of Mars

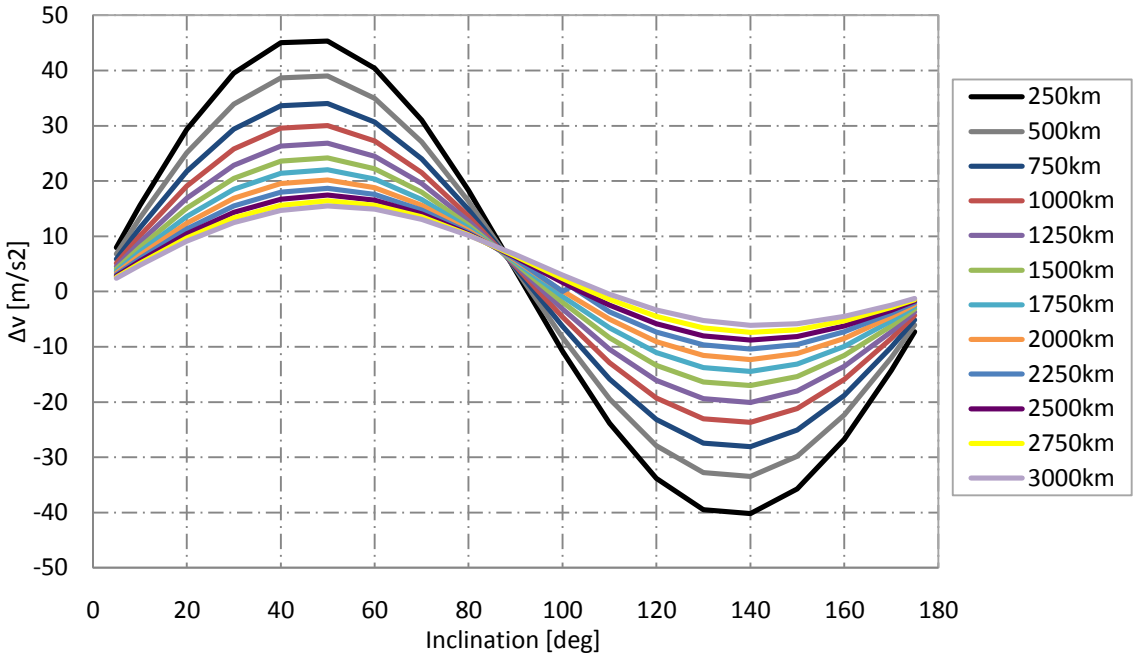

Figure 5 Required Δv per orbit for the extension of circular Sun-synchronous orbits of Mars

Figure 4 shows that circular sun-synchronous orbits with free selection of the inclination and altitude can be enabled using continuous out-of-plane acceleration. It is shown that orbits with inclinations around *90 degrees* require acceptable accelerations, and the further the inclination drifts from this region, the level of acceleration requires becomes infeasible using existing thruster technology.

2.3.2 Elliptical Sun-synchronous Orbits

If elliptical orbits are considered, two conditions can be combined to obtain sun-synchronous HEOs. These orbits use continuous out-of-plane acceleration to allow the ascending node angle to rotate to match the motion of the mean Sun, giving the sun-synchronous condition. Combined radial and transverse acceleration are then used to compensate for the applied normal acceleration and maintain the zero change in argument of periapsis condition essential to Molniya like orbits. The radial, transverse, normal and the total acceleration magnitude to achieve sun-synchronous HEOs of varying orbital period and inclination are given in Figure 6 for argument of pericentre values of *270 degrees* for a constant periapsis altitude of *800 km*. The Δv per orbit is also shown in Figure 7. It is noted that the same analysis is also conducted for an argument of periapsis value of *0 degrees*, these results are however similar to those for an argument of periapsis value of *270 degrees*, and so are not included in this paper. Comparison of these results shows that the value of the argument of pericentre does not significantly affect the level of acceleration required to achieve sun-synchronous HEOs as these accelerations are of the same order of magnitude.

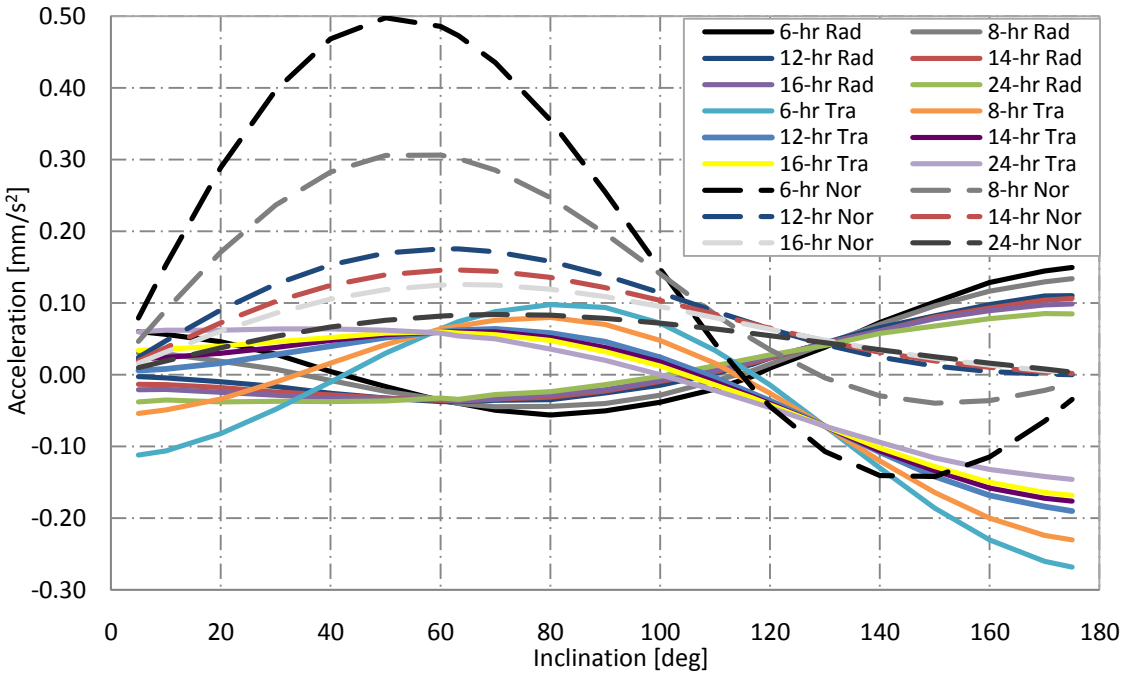

Figure 6 Required radial, transverse and normal acceleration to achieve sun-synchronous HEOs of varying period and inclination at Mars

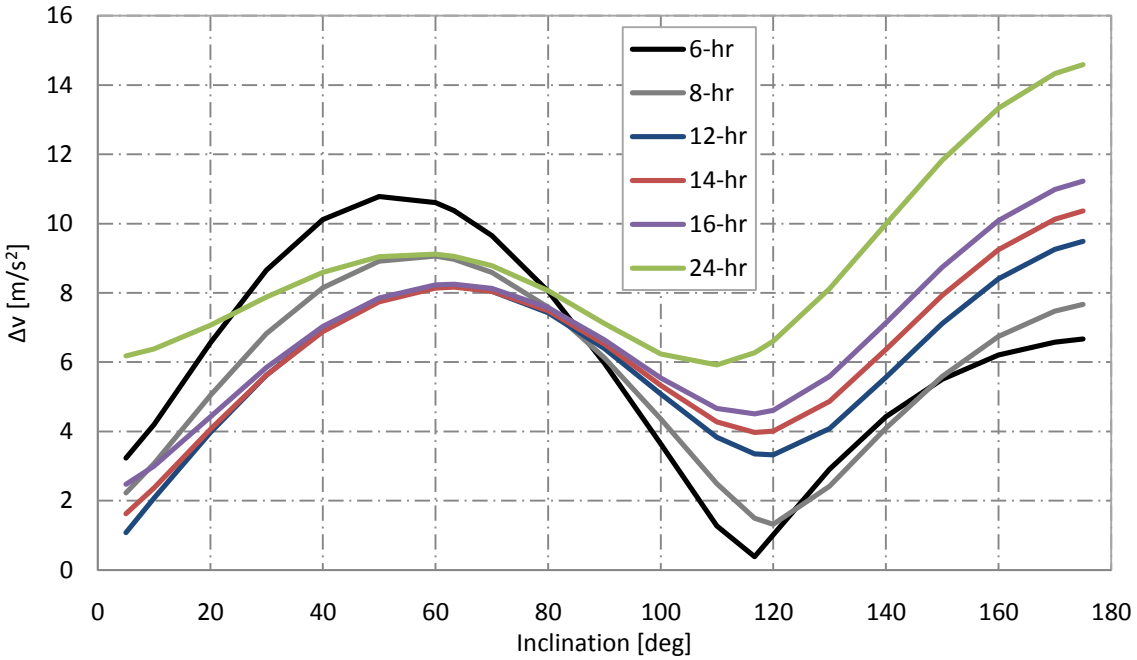

Figure 7 Required Δv per orbit to achieve sun-synchronous HEOs of varying period and inclination at Mars

From Figure 6 considering a 12 h orbit with an inclination of *90 degrees* requires a total acceleration magnitude of *0.31* and *0.15 mm/s*^{2} for argument of pericentre values of *0* and *270 degrees* respectively. Corresponding to initial thrust levels of *310* and *150 mN* respectively for a 1-ton spacecraft. Although these thrust levels are higher than that required for the orbits excluding the sun-synchronous condition, these levels are still within the capabilities of current thrusters. For example, the High Power Electric Propulsion (HiPEP) thruster which has undergone ground testing is capable of providing a maximum of *670 mN* [20] and test data from the Nuclear Electric Xenon Ion System (NEXIS) has also shown a maximum thrust level of *476 mN* [21].

2.3.3 Special Perturbations Solution

Similar to the extension of the critical inclination solutions, sun-synchronous HEOs are verified using numerical simulations. The oscillation of orbital elements for an orbit with an argument of pericentre of *270 degrees* are shown in Figure 8.

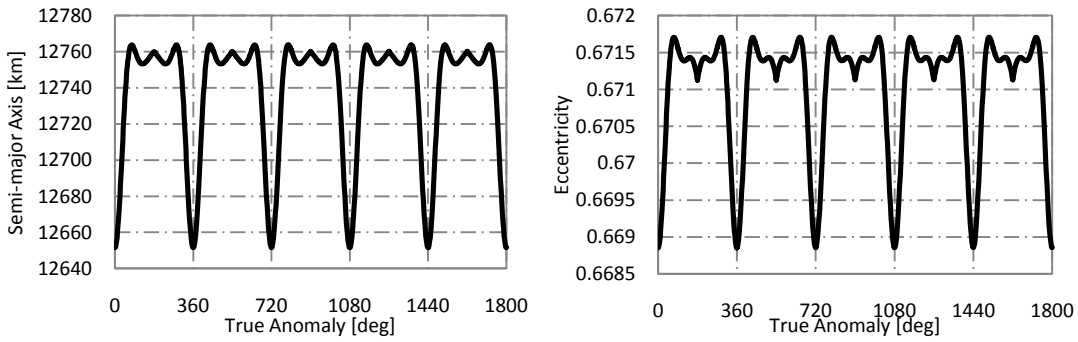

(a) (b)

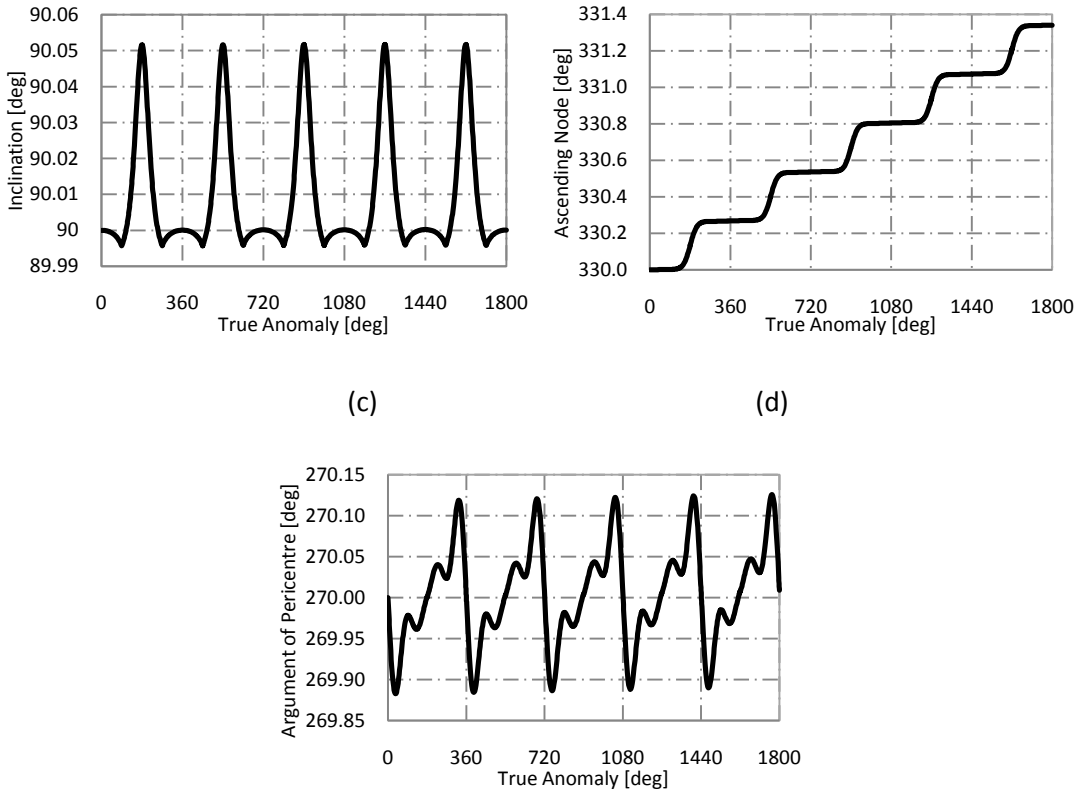

Figure 8 Oscillation of orbital elements over five orbital revolutions of a 12 h, *90 degree* inclination, sun-synchronous orbit at Mars (*270 degree* argument of periapsis) (a) Semi-major axis (b) Eccentricity (c) Inclination (d) Ascending node angle (e) Argument of pericentre

3. Venus and Mercury

As stated previously, like Earth and Mars, orbits at the critical inclination exist at Venus and Mercury, which can offer benefits for remote sensing; low-thrust propulsion can also therefore be used for the extension of these orbits.

Sun-synchronous orbits on the other hand do not naturally occur at Mercury or Venus due to the low reciprocal of flattening. Continuous acceleration is therefore considered to enable these orbits where they are otherwise not possible. Enabling sun-synchronous orbits could considerably enhance the opportunities for remote sensing at Venus and Mercury and the approximately constant illumination conditions and thus thermal environment can offer benefits both in terms of comparison of images and simplification of the spacecraft thermal design. Sections 3.1 and 3.2 present the full set of results for Venus, however as these results are similar to those of Mercury only specific examples are given in this case.

3.1 Highly-Elliptical Orbits

3.1.1 General Perturbations Solution

As the gravitational terms of Venus to the order of J_4 are of the same order of magnitude, development of orbits, like at Mars, must therefore include these higher order terms. The extension of the critical inclination at Venus is therefore performed by inserting Eqs. (13) – (15) into Eq. (14) integrating over one orbital revolution, setting the resulting expression equal to zero and solving for the radial and transverse accelerations required to alter the inclination. In these equations J_2, J_3 and J_4 are equal to $4.458x10^{-6}$, $-2.1082x10^{-6}$ and $-2.1471x10^{-6}$ respectively. As higher order gravity terms are significant in the case of Venus, the values of the critical inclination of orbits are dependent on the semi-major axis and eccentricity of the orbit. For example, a 12 h orbit with a pericentre altitude of *800 km* and apocentre altitude of *36,810 km* has critical inclinations of *85.3* and *94.7 degrees*, significantly differing from the natural critical inclination values derived for both Earth and Mars for the same orbital parameters. The radial, transverse and total acceleration magnitude required to alter these values of critical inclination to any inclination, for orbits of varying period and with constant pericentre altitude of *800 km* are presented in Figure 9, and the corresponding Δv per orbit is presented in Figure 10.

As Mercury is the least explored planet of the inner Solar System, detailed gravity field information is not yet available. Spacecraft motion about Mercury is therefore considered using gravity perturbations to the order of J_2 only, where J_2 is equal to $6x10^{-5}$ [22]. It is therefore expected that the accuracy of this work could be significantly enhanced by the inclusion of higher order gravity terms when these become available.

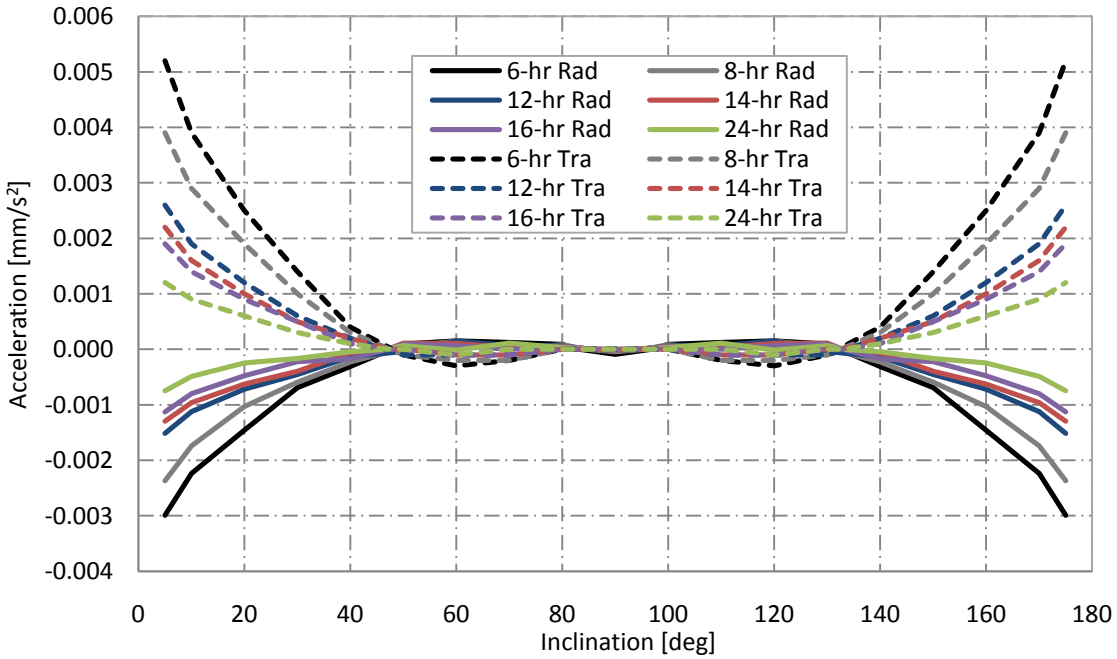

Figure 9 Required radial and transverse acceleration for the extension of highly-elliptical orbits at Venus

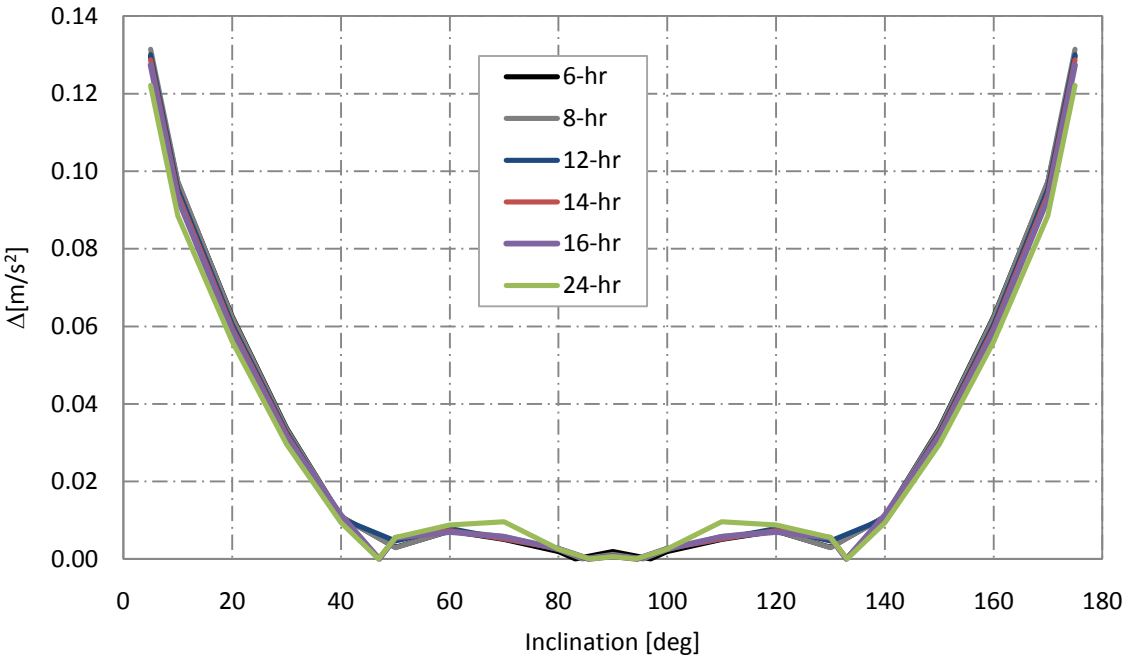

Figure 10 Required Δv per orbit for the extension of the critical inclination at Venus

Figure 9 shows the minimum radial and transverse components of acceleration to alter the critical inclination of the orbits to a wide range of possible values. It can be seen that to enable all of the considered orbits very small acceleration magnitudes are required. For example, considering a 12 h orbit with an inclination of *90 degrees* requires a total acceleration magnitude of $1.8x10^{-5}$ mm/s^2, which for a 1-ton spacecraft corresponds to a considerably low thrust level of *0.0185 mN*. This is compared with a total acceleration magnitude of *0.0012* mm/s^2 for the same orbit at Mercury, which equates to *1.2 mN* of thrust for a *1000 kg* spacecraft, which can be provided by the QinetiQ T5 thruster capable of providing thrust levels between *1* and *20 mN* [23].

3.1.2 Special Perturbations Solution

The general perturbations solutions are once again validated using a numerical model. A 12 h orbit is selected to demonstrate the special perturbations solution, results of which are given in Figure 11. Once again, the semi-major axis and eccentricity show oscillations over the orbit, but values return to the original value after each revolution of the spacecraft, and both the inclination and ascending node angle show no drift over the orbit. The argument of periapsis in both cases is shown to experience a small drift over the spacecraft orbit, however, this is only around $-6.3x10^{-4}$ *degrees* per orbit for an argument of periapsis values of *270 degrees*, which is thought to be an acceptable cost.

At Mercury, no variations are found in the inclination and ascending node angle, and oscillations in the semi-major axis, eccentricity and argument of pericentre are displayed with no variation shown over each orbital revolution.

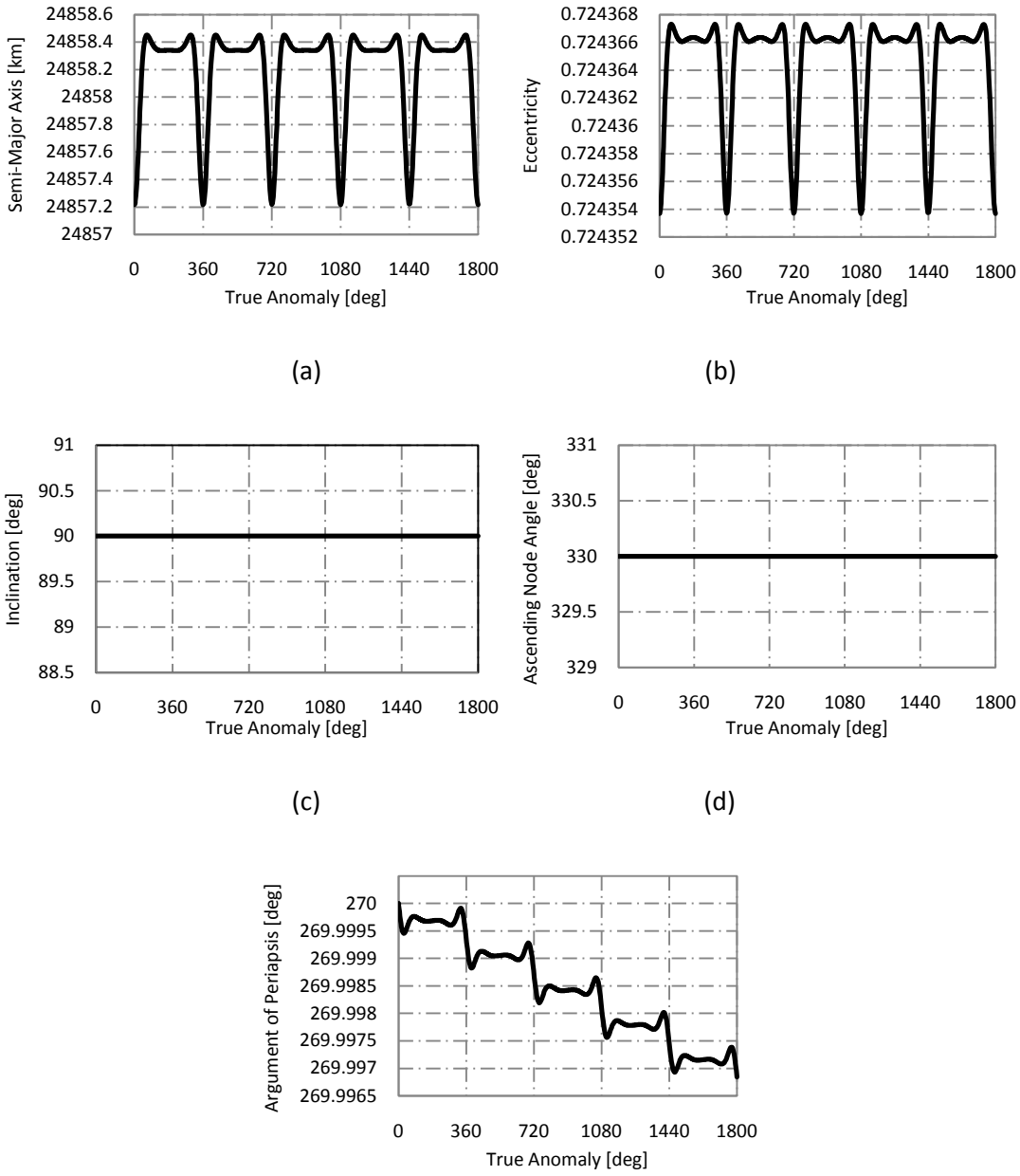

Figure 11 Oscillation of orbital elements over five orbital revolutions of a 12 h, *90 degree* inclination orbit at Venus (*270 degree* argument of periapsis) (a) Semi-major axis (b) Eccentricity (c) Inclination (d) Ascending node angle (e) Argument of pericentre

3.2 Sun-synchronous Orbits

As stated previously, natural sun-synchronous orbits do not occur at Venus. Sections 3.2.1 and 3.2.2 therefore present the use of continuous acceleration to enable circular and elliptical sun-synchronous orbits respectively, using low-thrust to achieve a rotation of the ascending node angle of 2π radians in *225 days*.

3.2.1 Circular Sun-synchronous Orbits

Eq. (17) is once again solved for the normal acceleration required to enable various circular sun-synchronous orbits around Venus and the result subsequently shown in Figure 12, the required acceleration is converted into the requisite Δv per orbit presented in Figure 13.

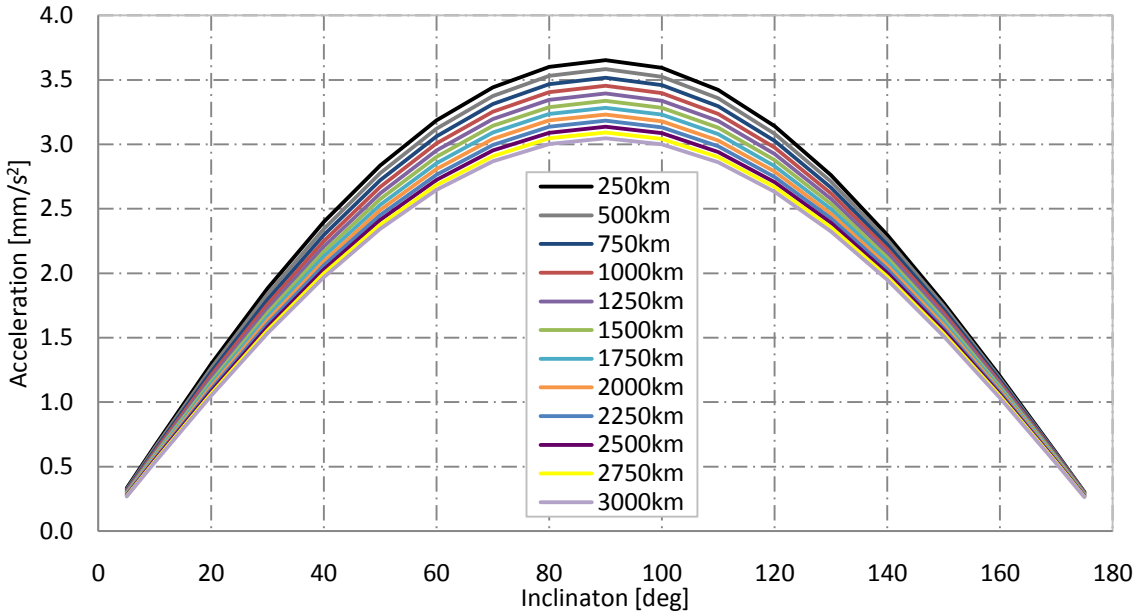

Figure 12 Normal acceleration required to enable circular sun-synchronous orbits of Venus

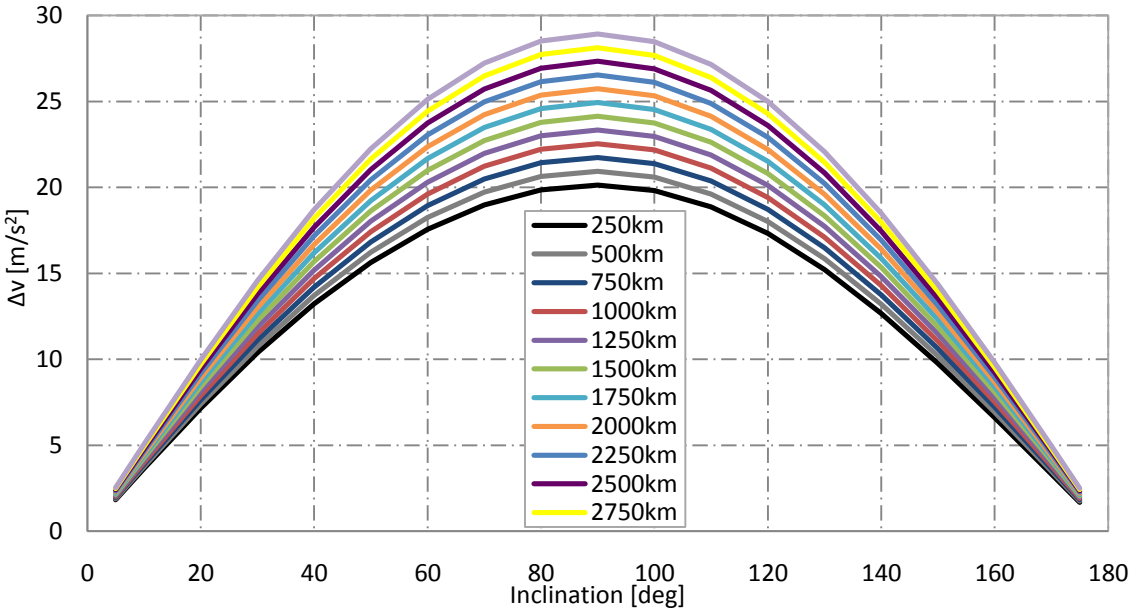

Figure 13 Required Δv per orbit to enable circular Sun-synchronous orbits of Venus

In order to enable circular sun-synchronous orbits a significant increase in acceleration magnitude is shown in Figure 12 from the extension of the critical inclination solutions. For example, a *1000 km* altitude orbit with an inclination of *90 degrees* requires a significant acceleration of *3.45 mm/s*^{2}.

The eccentric nature of Mercury's orbit around the Sun means that the required rate of change of the ascending node angle varies depending on the distance of the planet from the Sun. The required rate of change of the ascending node angle for a Sun-synchronous orbit is given as the specific angular momentum of Mercury with respect to the Sun divided by the square of the Mercury-Sun distance. The required rate of change of the ascending node angle therefore varies between $1.28x10^{-6}$ rad/s and $5.57x10^{-7}$ rad/s depending on Mercury's position from the Sun [16]. The maximum and minimum acceleration required to enable a Sun-synchronous, *1000 km*, altitude orbit inclined at *90 degrees* is *5.09 mm/s*^{2} and *2.21 mm/s*^{2} respectively. The required acceleration is therefore shown to be comparable for Mercury and Venus.

3.2.2 Elliptical Sun-synchronous Orbits

3.2.2.1 General Perturbations Solution

Once again, two conditions are combined to develop elliptical sun-synchronous orbits around Venus. Eq. (26) is used to determine the normal acceleration necessary to force the required rotation in the ascending node angle, and Eq. (21) is used to determine the radial and transverse acceleration necessary to ensure zero change in the argument of periapsis over the orbit. The required radial, transverse and normal accelerations are given in Figure 14 for an argument of periapsis value of *270 degrees*. Figure 15 shows the required Δv per orbit to achieve sun-synchronous HEOs, based on the total acceleration magnitude.

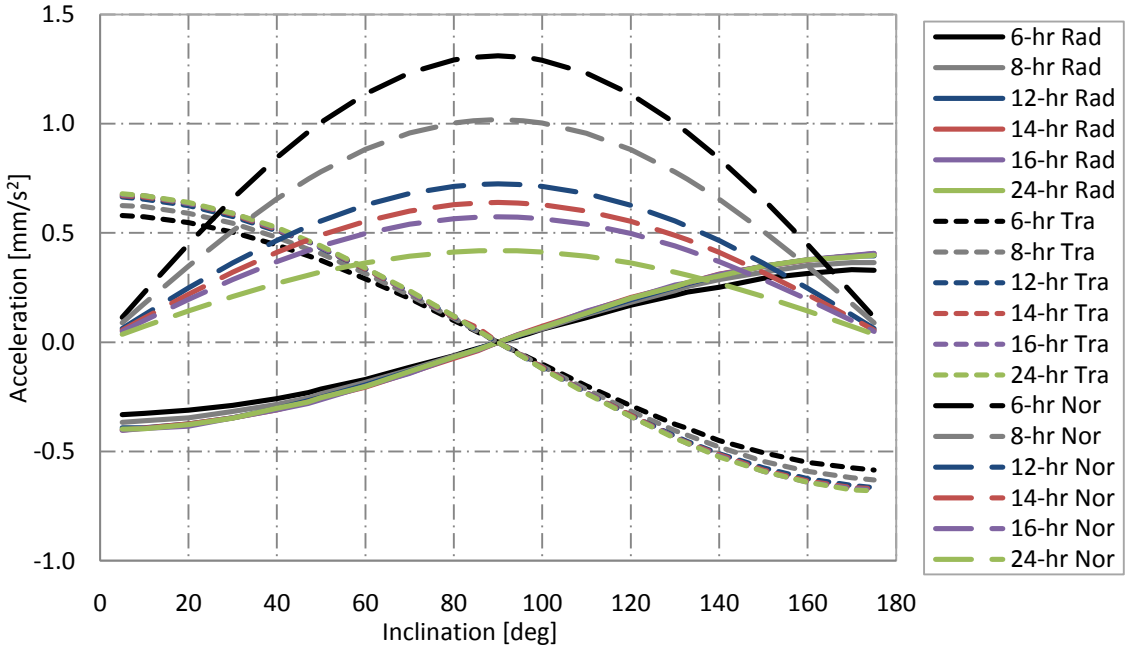

Figure 14 Required radial, transverse and normal acceleration to achieve sun-synchronous HEOs of varying period and inclination of Venus

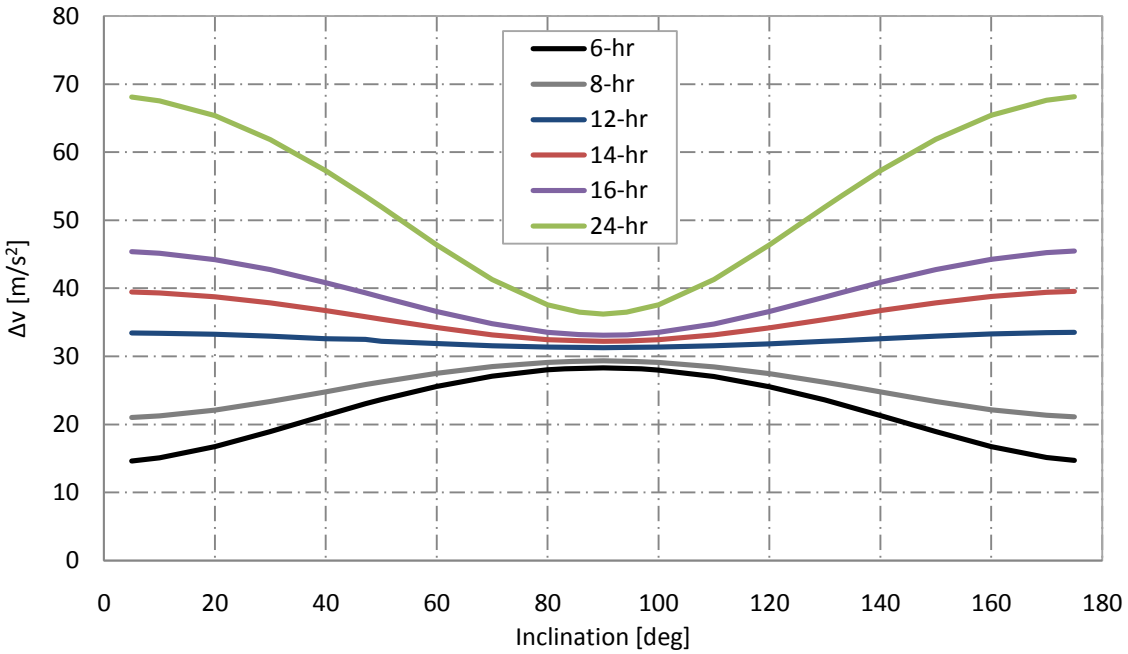

Figure 15 Required Δv per orbit to achieve sun-synchronous HEOs of varying period and inclination of Venus

Examination of Figure 14 illustrates the increase in acceleration magnitude required to enable elliptical sun-synchronous orbits over simply an extension of the critical inclination shown in Figure 9. Considering a 12 h orbit with an inclination of *90 degrees* requires an acceleration magnitude of *0.724 mm/s^2*, corresponding to *724 mN* of thrust for a *1000 kg* spacecraft, which is currently beyond the capabilities of existing low-thrust propulsion systems. Development in SEP thruster capabilities is therefore required before these orbits can become feasible. Once again the results obtained for Mercury are comparable to Venus, with a maximum and minimum acceleration magnitude of *1.30 mm/s^2* and *0.57 mm/s^2* required to achieve a 12 h elliptical sun-synchronous orbit inclined at *90 degrees* to the equator.

3.2.2.2 Special Perturbations Solution

Figure 16 gives the variation of orbital elements for a 12 h elliptical sun-synchronous orbit at Venus with an argument of periapsis value of *270 degrees* as a result of the numerical simulation. The required change in ascending node angle of *0.8 degrees* per orbit is shown to be achieved, with negligible changes in semi-major axis, eccentricity and inclination over each orbital revolution. As was the case with the extension of the critical inclination at Venus (Figure 11), a small drift in the argument of periapsis is found when enabling elliptical sun-synchronous orbits. A drift in ω of *1.12x10^{-3} degrees* per orbit is determined, which equates to around *0.5 degrees* per Venusian year. This is once again expected to be an acceptable cost. The slight increase in the drift of the argument of periapsis exhibited for elliptical sun-synchronous orbits at Venus is cause by the oscillation of the semi-major axis, eccentricity and inclination in this case, which has an impact on the argument of periapsis. The analytical solution makes the assumption that the changes in all elements are zero; the numerical simulation however indicates that in this case this assumption begins to break down.

At Mercury, negligible changes in the semi-major axis, eccentricity and inclination are once again shown, with a rotation of the ascending node shown to agree with the analytical solutions with a rotation of around *2 degrees* per orbit. However, as was the case with Venus, a small drift in the argument of periapsis is exhibited, with a drift of around *0.01 degrees* exhibited per orbit. Although a drift is shown, this amounts to less than *2 degrees* per Mercury year respectively, which is expected to be an acceptable cost. This drift is again caused by the oscillation in the semi-major axis, eccentricity and inclination in the numerical solution, which is assumed to be negligible in the analytical solution.

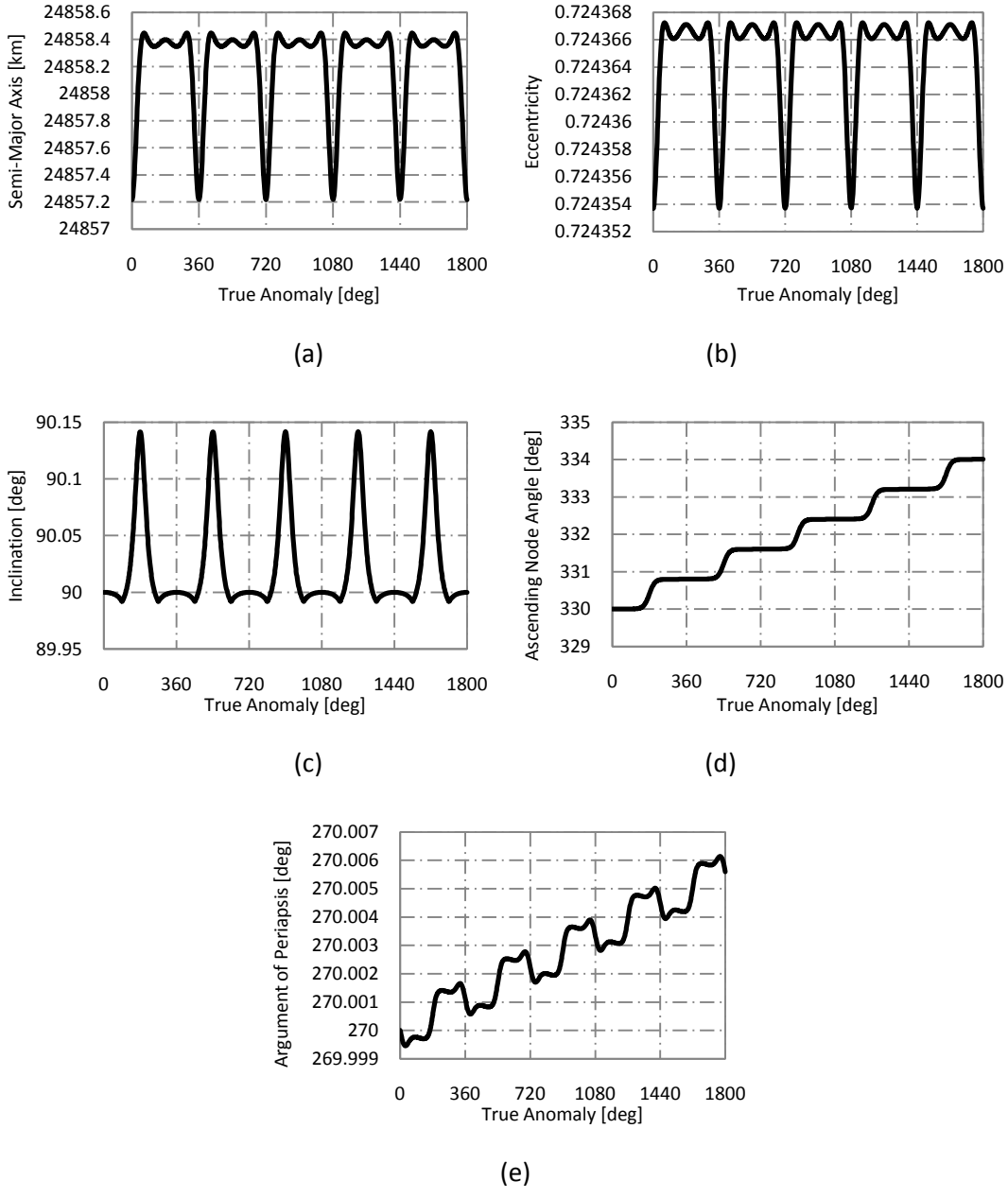

Figure 16 Oscillation of orbital elements over five orbital revolutions of a 12 h, *90 degree* inclination, sun-synchronous orbit at Venus (*270 degree* argument of periapsis) (a) Semi-major axis (b) Eccentricity (c) Inclination (d) Ascending node angle (e) Argument of pericentre

4. Conclusion

Continuous low-thrust propulsion has been shown to extend highly-elliptical orbits at the critical inclination at Mars, Mercury and Venus, which at Mercury and Mars can be achieved using existing electric propulsion systems; to extend sun-synchronous orbits at Mars which can again be achieved with current thrusters; and to enable circular and elliptical sun-synchronous orbits at Mercury and Venus, which otherwise do not naturally occur these however are likely to require significant development of electric propulsion systems before becoming feasible. These newly proposed orbits could however significantly enhance the opportunities for remote sensing of the inner planets of the Solar System and the near constant illumination conditions offer benefits in terms of simplified instrument design as a result of the predictable thermal environment and to enable repeat observations of a target over an extended period under similar illumination conditions.

5. References

1. Smith, J. C., and Bell, J. M. "2001 Mars Odyssey Aerobraking," *Journal of Spacecraft and Rockets* Vol. 42, No. 3, 2005, pp. 406-415
2. Chicarro, A., Martin, P., and Trautner, R. "The Mars Express Mission: An Overview." ESA, ESTEC, Noordwijk, The Netherlands, 2004.
3. Zurek, R. W., and Smrekar, S. E. "An overview of the Mars Reconnaissance Orbiter (MRO) science mission," *Journal of Geophysical Research* Vol. 112, No. E05S01, 2006.doi: 10.1029/2006JE002701
4. Sellers, P. J., Garvin, J. B., Kinney, A. L., Amato, M. J., and White, N. E. "A Vision for the Exploration of Mars: Robotic Precursors Followed by Humans to Mars Orbit in 2033," *Concepts and Approaches for Mars Exploration*. Houston Texas, 2012.
5. Squyres, S. "Vision and Voyages For Planetary Science in the Decade 2013-2022." 2011.
6. Jai, B., Wenkert, D., Hammer, B., Carlton, M., Johnston, D., and Halbrook, T. "An Overview of Mars Reconnaissance Orbiter Mission and Operations Challenges," *AIAA Space 2007 Conference & Exposition*. Long Beach, California, 2007.
7. Lyons, D. T., Beerer, J. G., Esposito, P., and Johnston, D. M. "Mars Global Surveyor: Aerobraking Mission Overview," *Journal of Spacecraft and Rockets* Vol. 36, No. 3, 1999, pp. 307-313
8. Liu, X., Baoyin, H., and Ma, X. "Extension of the Critical Inclination," *Astrophysics and Space Science* Vol. 334, No. 1, 2011, pp. 115 - 124
9. Leipold, M., Borg, E., Linger, S., Pabsch, A., Sachs, R., and Seboldt, W. "Mercury Orbiter with a Solar Sail Spacecraft," *Acta Astronautica* Vol. 35, No. 1, 1995, pp. 635-644
10. Anderson, P., and Macdonald, M. "Extension of Highly Elliptical Earth Orbits using Continuous Low-Thrust Propulsion," *Journal Guidance Control and Dynamics* Vol. 36, No. 1, 2013, pp. 282-292
11. Anderson, P., and Macdonald, M. "Sun-Synchronous Highly Elliptical Orbits using Low-Thrust Propulsion," *Journal of Guidance, Control and Dynamics*, 2012,
12. Circi, C., Ortore, E., Bunkheila, F., and Ulivieri, C. "Elliptical Multi-Sun-Synchronous Orbits for Mars Exploration," *Celestial Mechanics and Dynamical Astronomy* Vol. 114, No. 3, 2012, pp. 215-227
13. Ortore, E., Circi, C., Bunkheila, F., and Ulivieri, C. "Earth and Mars Observation using Periodic Orbits," *Advances in Space Research* Vol. 49, No. 1, 2012, pp. 185-195

14. Bate, R. R., Mueller, D. D., and White, J. E. *Fundamentals of Astrodynamics*. New York: Dover 1971.
15. Fortescue, P., Stark, J., and Swinerd, G. *Spacecraft Systems Engineering*. New York: Wiley, 2003.
16. Macdonald, M., and McInnes, C. R. "Analytical Control Laws for Planet-Centered Solar Sailing," *Journal of Guidance, Control and Dynamics* Vol. 28, No. 5, 2005, pp. 1038-1048
17. Brophy, J. R., Kakuda, R. Y., Polk, J. E., Anderson, J. R., Marcucci, M. G., Brinza, D., Henry, M. D., Fujii, K. K., Mantha, K. R., Stocky, J. F., Sovey, J., Patterson, M., Rawlin, V. K., Hamley, J., Bond, T., Christensen, J., Cardwell, H., Benson, G., Gallagher, J., Matranga, M., and Bushway, D. "Ion Propulsion System (NSTAR) DS1 Technology Validation Report," *JPL Publication 00-10*. 2000.
18. Walker, M. J. H., Ireland, B., and Owens, J. "A set of Modified Equinoctial Orbital Elements," *Celestial Mechanics* Vol. 36, No. 4, 1985.doi: 10.1007/BF01227493
19. Dormand, J. R., and Prince, P. J. "A family of embedded Runge-Kutta formulae," *Journal of Computational and Applied Mathematics and Statistics* Vol. 6, No. 1, 1980, pp. 19-26.doi: 10.1016/0771-050X(80)90013-3
20. Foster, J. E., Haag, T., Patterson, M., Williams, G. J., Sovey, J. S., Carpenter, C., Kamhawi, H., Malone, S., and Elliot, F. "The High Power Electric Propulsion (HiPEP) Ion Thruster," 2004,
21. Randolph, T. M., and Polk, J. E. "An overview of the Nuclear Electric Xenon Ion System (NEXIS) Activity," *40th AIAA/ASME/SAE/ASEE Joint Propulsion Conference*. Fort Lauderdale, Florida, 2004.
22. Anderson, D. J., Colombo, G., Esposito, P. B., Lau, E. L., and Trager, G. B. "The Mass, Gravity Field and Ephemeris of Mercury," *Icarus* Vol. 71, No. 3, 1987, pp. 337 - 349.doi: 10.1016/0019-1035(87)90033-9
23. Edwards, C. H., Wallace, N. C., Tato, C., and Put, C. V. "The T5 Ion Propulsion Assembly for Drag Compensation on GOCE," *Second International GOCE User Workshop "GOCE, The Geoid and Oceanography"*. Frascati, Italy, 2004.